Optical phase-space modes, self-focusing, and the wavelength as tunable

2015 Phys. Scr. 90 128003

(http://iopscience.iop.org/1402-4896/90/12/128003)

IOP Publishing | Royal Swedish Academy of Sciences Physica Scripta

Phys. Scr. **90** (2015) 128003 (5pp) doi:10.1088/0031-8949/90/12/128003

Invited Comment

Optical phase-space modes, self-focusing, and the wavelength as tunable $\hbar$

A M Zheltikov[1,2,3]

[1] Department of Physics and Astronomy, Texas A&M University, College Station TX 77843, USA
[2] Physics Department, International Laser Center, M.V. Lomonosov Moscow State University, Moscow 119992, Russia
[3] Russian Quantum Center, ul. Novaya 100, Skolkovo, Moscow Region 143025, Russia

E-mail: zheltikov@physics.tamu.edu

Received 19 June 2015, revised 19 September 2015
Accepted for publication 7 October 2015
Published 11 November 2015

Abstract

The Hamiltonian optics notion of phase-space modes is shown to be central to understanding self-focusing, multiple filamentation, and the λ^2 scaling of the self-focusing threshold with the radiation wavelength λ.

Keywords: self-focusing, ultrafast optics, nonlinear optics

(Some figures may appear in colour only in the online journal)

The wavelength is one of the key variables in optical science. The properties of materials and regimes of light–matter interactions can vary dramatically from one wavelength range to another. Ultrafast laser technologies provide a vast arsenal of tools to understand the optical response of matter as a function of the wavelength. With the advent of efficient laser sources of ultrashort pulses in the mid-infrared [1–3], ultrafast nonlinear optics rapidly expands beyond experiments with a near-infrared driver, revealing unique regimes of optical-harmonic generation [1, 4], laser-induced filamentation [2, 3, 5, 6], and high-brightness x-ray generation [7], as well as shedding light on unusual properties of materials in the mid-infrared [8].

Research into the strong-field physics behind light–matter interactions reveals physically significant tendencies in the optical response of matter as a function of the laser driver wavelength λ. It is instructive to divide these wavelength scaling laws into two classes. The scaling laws of the first class deal with electron wave-packet dynamics. In many important cases, a quasi-classical treatment provides an adequate description of this dynamics, leading to a λ^2 scaling for the ponderomotive energy U_p of an electron wave packet, as dictated by the Newtonian mechanics [9]. This scaling is instrumental in understanding laser electron acceleration, dynamics of recolliding photoelectrons, and high-harmonic generation. The $U_p \propto \lambda^2$ scaling suggests the ways toward a higher spatial resolution in attosecond molecular imaging [10–12] and higher coherent x-ray yields in high-harmonic generation. The semiclassical electron wave-packet dynamics within the field half-cycle has been found to be the key factor behind the wavelength scaling of optical nonlinearities, explaining the difficulties of the perturbative, phenomenological treatment of ultrafast nonlinear phenomena in terms of nonlinear susceptibilities in the long-wavelength range [8].

In this work, we focus on the scaling laws of the second class. The physics behind these laws is different, as they reflect the wave aspects of light–matter interactions and relate to both linear and nonlinear propagation effects. Here, we offer a Hamiltonian-optics perspective on these phenomena, highlighting similarities between the wave equation for optical fields and equations for the quantum-mechanical wave function. When put in the context of commutation relations and related Heisenberg-type uncertainty, the role of the radiation wavelength λ in optical phenomena is similar to the role of the Planck constant $\hbar$ in quantum mechanics, as both defining the granularity of the phase space of the relevant canonical variables. Nonlinear-optical propagation effects, such as self-focusing, are shown to probe this λ-dependent phase-space granularity, visualizing the spatial modes of light through a breakup of a coherent beam into N filaments, with

N controlled by the number of self-trapped spatial modes within the beam. This perspective sheds light on the self-focusing threshold P_s as the peak power needed to trap a single spatial mode of an optical field, with the λ^2 dependence of the phase-space volume of this mode translating into the celebrated λ^2 scaling of P_s.

The starting point of our analysis is the one-dimensional time-dependent Schrödinger equation for the wave function $\Psi(\mathbf{r}, t)$,

$$\hat{H}\Psi(\mathbf{r}, t) = \left[\frac{\hat{\mathbf{p}}^2}{2m} + V(\mathbf{r}, t)\right]\Psi(\mathbf{r}, t), \tag{1}$$

where

$$\hat{H} = \mathrm{i}\hbar\frac{\partial}{\partial t}, \tag{2}$$

$$\hat{\mathbf{p}} = -\mathrm{i}\hbar\nabla, \tag{3}$$

m is the mass, and $V(\mathbf{r}, t)$ is the potential energy.

Equations of this class are known to describe a broad class of optical processes. Specifically, dynamics of an optical beam in a medium with a third-order optical nonlinearity can be approximately described with a scalar parabolic wave equation [13]

$$2\mathrm{i}k_0\frac{\partial E}{\partial z} + \frac{\partial^2 E}{\partial x^2} + \frac{\partial^2 E}{\partial y^2} + 2k_0 kE = 0, \tag{4}$$

where E is the transverse component of the electric field, $k \equiv k(x, y) = 2\pi n(x, y)/\lambda$, $k_0 \equiv k(0, 0)$, $n(x, y)$ is the transverse profile of the refractive index.

Following the insight by Fock [14], we use a replacement

$$\hbar \to \lambda\!\!\!^{-}, \; t \to z, \; m/\hbar \to k_0, \; V(x, y) \to n(x, y), \tag{5}$$

to reduce equations (4) to (1), with the Hamiltonian and momentum operators defined as

$$\hat{H} = \mathrm{i}\lambda\!\!\!^{-}\frac{\partial}{\partial z}, \tag{6}$$

$$\hat{p}_x = -\mathrm{i}\lambda\!\!\!^{-}\frac{\partial}{\partial x}, \quad \hat{p}_y = -\mathrm{i}\lambda\!\!\!^{-}\frac{\partial}{\partial y}. \tag{7}$$

For a medium with a third-order optical nonlinearity, with $n(x, y) = n_0 + n_2 I(x, y)$, where n_0 is the field-free refractive index, n_2 is the nonlinear refractive index, and $I(x, y)$ is the field intensity profile, this nonlinear Schrödinger equation (NSE) describes nonlinear self-action effects [15, 16], including the self-focusing of a laser beam as a whole and beam breakup due to modulation instability (MI).

Perhaps, the most intriguing aspect of equation (5) is that it reveals interesting parallels between the role of $\hbar$ in quantum mechanics and $\lambda\!\!\!^{-}$ in optics [14, 17]. The physical significance of this observation is best appreciated in the context of the original Planck's definition of $\hbar$ as the size of an elementary phase-space cell. To illustrate how the wavelength λ limits the elementary phase-space volume in optics, we consider a Gaussian beam of radiation with a beam radius w_0 (figure 1(a)). Diffraction-induced divergence of this beam is characterized by a divergence angle $\theta \approx \lambda(\pi w_0)^{-1}$. The

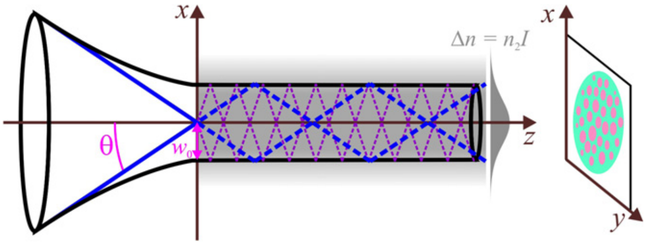

Figure 1. Self-focusing couples a freely diffracting laser beam to a group of spatial modes (solid and dashed lines) trapped by the refractive index change $\Delta n = n_2 I$. The interference of these modes, partially randomized by stochastic processes involved in beam dynamics, including ionization, gives rise to a speckle pattern.

phase-space mode volume, Ξ_m, defined as a product of the beam area $S_m = \pi w_0^2$ and the solid angle of beam divergence, $\Omega_m = \pi\theta^2$, is then a constant,

$$\Xi_m = S_m\Omega_m = \lambda\!\!\!^{-2}, \tag{8}$$

controlled by the radiation wavelength.

Equation (8) is a manifestation of more general relations, reflecting the fundamental mode properties of optical fields. Indeed, with time t replaced by the longitudinal coordinate z, as in equations (1) and (4), the Fermat's principle in optics becomes mathematically identical to the Hamilton's principle in mechanics [17]. Optical rays can then be described as trajectories of classical particles, while optical waves can be treated similar to quantum-mechanical wave functions. With the Hamiltonian formulation of the Fermat's principle,

$$\int_{z_1}^{z_2} L(x, y, x', y', z)\mathrm{d}z = \min, \tag{9}$$

where

$$L(x, y, x', y', z)\mathrm{d}z = n(x, y, z)\left[1 + x'^2 + y'^2\right]^{1/2} \tag{10}$$

is the Lagrangian,$x' = \mathrm{d}x/\mathrm{d}z$, $y = \mathrm{d}y/\mathrm{d}z$, and $n(x, y, z)$ is the refractive index, the generalized momenta conjugate to the variables x and y are given by [17]

$$p_x = \frac{\partial L}{\partial x'} = n \sin\alpha_x, \tag{11}$$

$$p_y = \frac{\partial L}{\partial y'} = n \sin\alpha_y, \tag{12}$$

with α_x and α_y being the angles defining the ray direction.

The Liouville theorem applied to a bundle of rays requires the phase-space volume filled with points representing this bundle to remain constant. The constancy of the phase-space mode volume Ξ_m in equation (8) can now be viewed as a consequence of the Liouville theorem applied to the x, y, p_x, p_y phase space. The fundamental significance of this argument is, perhaps, best appreciated in terms of the second law of thermodynamics, which prohibits any linear optical system to change the phase-space volume of a spatial mode. Furthermore, with momenta p_x and p_y defined in accordance with equation (7), which offers a quantum version of equations (11) and (12), the canonically conjugate variables x, y, p_x, and p_y satisfy commutation relations

$xp_x - p_x x = i\lambda\!\!\!^{-}$ and $yp_y - p_y y = i\lambda\!\!\!^{-}$, which translate into the Heisenberg-type uncertainty, $(w_0\theta)^2 \geqslant (\lambda/\pi)^2$, in perfect agreement with equation (8).

When written in a canonical form,

$$ik\frac{\partial E}{\partial z} + \frac{1}{2}\Delta_\perp E + \eta|E|^2 E = 0, \tag{13}$$

the NSE reveals two physically significant integrals of motion [16]—the energy integral,

$$Q = \frac{1}{2k^2}\int_{-\infty}^{\infty}\left[\left(\Delta_\perp E\right)^2 - \eta|E|^4\right]d^2\rho, \tag{14}$$

and the integral of the number of particles,

$$N = \int_{-\infty}^{\infty}|E|^2 d^2\rho, \tag{15}$$

where ρ is the radius vector in the xy-plane.

With the physical units restored, the N integral of equation (15) can be represented as $N = P/P_s$, where $P_s = \lambda^2(2\pi n_0 n_2)^{-1}$ is the critical power of self-focusing [15, 16, 18]. It is instructive to view this parameter as the number of modes trapped by the refractive index change $\Delta n = n_2 I$ induced by a laser beam with an on-axis field intensity I [19]. With $P = P_s$, one has $N = 1$, showing that the refractive index change induced by a laser beam with $P = P_s$ is sufficient to confine only one spatial mode. The λ^2 scaling of the self-focusing threshold P_s can now be understood as a reflection of the $\Xi_m \propto \lambda^2$ scaling of the phase-space volume of spatial modes.

We will show now that this spatial-mode perspective on self-focusing offers useful insights into small-scale self-focusing and multiple filamentation phenomena [20, 21], as well as into the relation of these effects to spatial MI [22]. In a canonical, textbook picture of multiple filamentation dynamics, a laser beam with a high peak power $P > P_s$ undergoes small-scale self-focusing, forming, typically for $P \sim 3 \div 7P_s$ [20, 21, 23–25], multiple filaments as a result of instability of a laser beam with respect to a small-amplitude harmonic modulation. While MI is a universal physical factor behind small-scale self-focusing, the specific statistics of fluctuations across the laser beam and along the nonlinear medium has to be taken into consideration for an adequate description of multiple filamentation [26, 27].

The canonical theory of spatial modulation instabilities [22] offers a useful tool for simple and reasonably accurate estimates on a typical size of filaments and a typical propagation length needed for the buildup of small-scale self-focusing [27]. However, this theory does not help to distinguish between small-scale self-focusing and formation of multiple filaments. As a result, within a broad range of experimental conditions, this approach fails to explain the beam profiles of a high-peak-power, $P > P_s$ laser pulses, which often radically differ from a manifold of isolated, well-formed filaments (figures 2(a) and (b)).

To address this question, we take a Hamiltonian optics phase-space perspective on self-focusing by viewing this process as a result of coupling of a free-space laser beam into the modes of a waveguide formed by the refractive index change $\Delta n = n - n_0 = n_2 I$ induced by a laser beam with an on-axis field intensity I in a medium with a field-free refractive index n_0. The interference of these modes, partially randomized by stochastic processes involved in beam dynamics, including ionization, will give rise to a speckle pattern (figure 1(b)) exactly as the one observed in figure 2(a). The highest order spatial modes, propagating at a critical angle $\theta_c \approx \left(n^2 - n_0^2\right)^{1/2}$ relative to the beam axis, will then translate into the smallest speckles, whose size is given by $d \approx \lambda/\sin\theta_c \approx \lambda\left(n^2 - n_0^2\right)^{-1/2} \approx \lambda(2n_0 n_2 I)^{-1/2}$.

It is instructive to compare this result with predictions of the Bespalov–Talanov (BT) theory of small-scale self-focusing [22]. According to this theory, in a strong laser field, a steady-state wave $E_0 = B_0\exp(-i\Phi)$, with $\Phi = \omega n_2(2c)^{-1}|B_0|^2 z$, becomes unstable with respect to a small harmonic perturbation $E_1 = B_1(z)\cos(2\pi qr)\exp(-i\Phi)$, where $r = (x^2 + y^2)^{1/2}$ and q is the transverse wave number. The maximum value of MI gain $K(q) = |B_1(z)|/|B_0|$ is achieved [22] for perturbations with the phase

$$\phi_{\max} = -\frac{3\pi}{4} - \frac{1}{2}\arctan\left[\frac{Q - \Phi}{\kappa Q}\tanh(\kappa Q)\right] + \pi m, \tag{16}$$

and is given by

$$K_{\max} = \frac{\Phi}{\kappa Q}\sinh(\kappa Q) + \left\{1 + \left[\frac{\Phi}{\kappa Q}\sinh(\kappa Q)\right]^2\right\}^{1/2}, \tag{17}$$

where $\kappa = 2\pi^2 q^2 c(n_0\omega)^{-1}z$, $Q = (2\Phi\kappa^{-1} - 1)^{1/2}$, and m is an integer.

The transverse wave number of the highest order spatial modes in our analysis presented above, $k_\perp \approx 2\pi(2n_0 n_2 I)^{1/2}/\lambda$, exactly reproduces the result of the BT theory for the transverse wave number of harmonic modulation that corresponds to the maximum MI gain. The gain and the buildup lengths of the θ_c modes in the Δn waveguide are thus also equal to the gain and buildup lengths of the maximum-gain modes in the BT theory. Finally, the number of speckles in a beam, estimated as $N_s \approx 4w_0^2/d^2 \approx 4\pi^{-2}(P/P_s)$ (figure 1(b)), agrees reasonably well with $N = P/P_s$.

Figure 3 displays the angular spectrum of a laser beam with a peak power $P \approx 3$ GW, a pulse width $\tau \approx 30$ fs, and a central wavelength $\lambda = 800$ nm transmitted through a 360 μm thick silica plate normalized to the angular spectrum of the input field. The solid line presents the results of numerical simulations performed with the use of the relevant three-dimensional generalized NSE [20, 21, 27–29]. The dashed line shows the increment of a spatial mode with a transverse wave number $k_\perp = 2\pi q$ calculated using the BT theory. With $I \approx 6$ TW cm^{-2} for the parameters of laser pulses used in simulations, the size of speckles corresponding to the maximum-gain modes is $d \approx 12\,\mu$m. The results of numerical simulations are seen to agree well with our

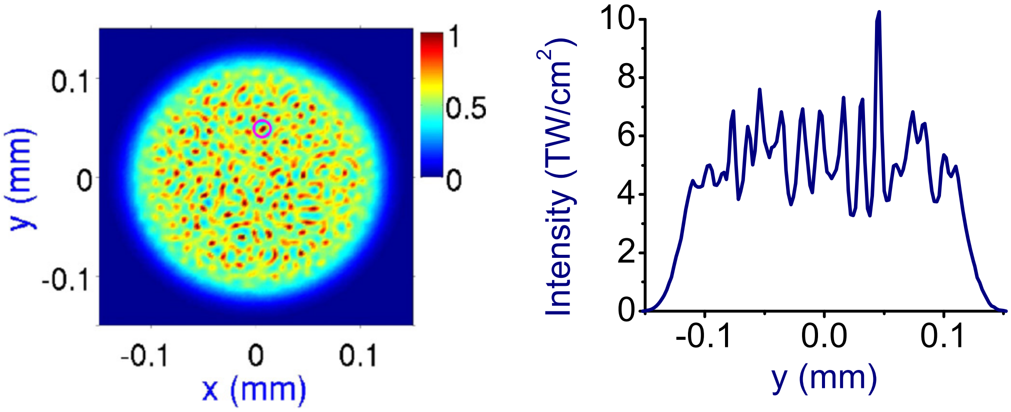

Figure 2. The field intensity profile within the laser beam with $P \approx 3$ GW, $\tau \approx 30$ fs, and $\lambda = 800$ nm transmitted through a 360 μm thick silica plate. A Gaussian noise with a standard deviation of 0.0185 is applied to the beam profile to mimic optical inhomogeneities. (b) The one-dimensional cut of the field intensity profile shown in panel (a).

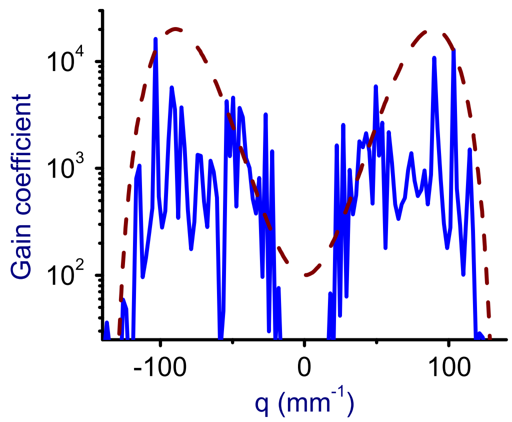

Figure 3. The angular spectrum of a laser beam with $P \approx 3$ GW, $\tau \approx 30$ fs, and $\lambda = 800$ nm transmitted through a 360 μm thick silica plate normalized to the angular spectrum of the input field: (solid line) numerical simulations performed with the use of the relevant three-dimensional generalized NSE, (dashed line) the gain of a spatial mode calculated as a function of its transverse wave number $q = k_\perp/2\pi$ using the BT theory.

qualitative arguments. Both numerical simulations and BT theory calculations yield gain spectra featuring a cutoff around $q_{max} \approx 90\ \mathrm{mm}^{-1}$, corresponding to transverse inhomogeneities of the beam profile with a typical size of $d \approx 1/q_{max} \approx 11\ \mu$m. Within longer propagation lengths, hot spots that arise across the beam due to the interference of spatial modes tend to evolve toward the formation of isolated filaments. However, far-field speckle patterns similar to the one presented in figure 2(a) visualize the breakup of a laser beam into confined spatial modes regardless of whether isolated filaments had time and space to build up as a part of nonlinear beam dynamics.

To summarize, we have shown that the Hamiltonian optics concept of phase-space modes is central to understanding self-focusing, multiple filamentation, and the λ^2 scaling of the self-focusing threshold with the radiation wavelength λ. In Hamiltonian optics, λ plays a part of the Planck constant $\hbar$ in commutation relations and, hence, in the Heisenberg-type uncertainty for the canonical variables. However, unlike $\hbar$, the wavelength is tunable, defining a phase space with a variable granularity. Self-focusing is shown to probe this λ-dependent phase-space granularity, visualizing the spatial modes of light through a breakup of a coherent beam into N filaments, with N controlled by the number of self-trapped spatial modes within the beam. This perspective sheds light on the multiple-filamentation dynamics and on the self-focusing threshold P_s as the peak power needed to trap a single spatial mode of an optical field, with the λ^2 dependence of the phase-space volume of this mode translating into the celebrated λ^2 scaling of P_s.

Acknowledgments

Stimulating discussions with and invaluable help from AA Voronin are gratefully acknowledged. This research was supported in part by the Russian Foundation for Basic Research (project nos.14-02-90030, and 14-29-07182) and the Welch Foundation (Grant No. A-1801). Research into the nonlinear optics in the mid-infrared has been supported by the Russian Science Foundation (project no. 14-12-00772).

References

[1] Popmintchev T *et al* 2012 Bright coherent ultrahigh harmonics in the keV x-ray regime from mid-infrared femtosecond lasers *Science* **336** 1287–91
[2] Mitrofanov A V *et al* 2015 Mid-infrared laser filaments in the atmosphere *Sci. Rep.* **5** 8368
[3] Mitrofanov A V *et al* 2015 Subterawatt femtosecond pulses in the mid-infrared range: new spatiotemporal dynamics of high-power electromagnetic fields *Phys.—Usp.* **58** 89–94
[4] Kartashov D, Ališauskas S, Pugžlys A, Voronin A A, Zheltikov A M and Baltuška A 2012 Third- and fifth-harmonic generation by mid-infrared ultrashort pulses: beyond the fifth-order nonlinearity *Opt. Lett.* **37** 2268–70
[5] Kartashov D, Ališauskas S, Pugžlys A, Voronin A, Zheltikov A, Petrarca M, Béjot P, Kasparian J, Wolf J-P and Baltuška A 2012 White light generation over three octaves by femtosecond filament at 3.9 μm in argon *Opt. Lett.* **37** 3456–8

[6] Kartashov D, Ališauskas S, Pugžlys A, Voronin A, Zheltikov A, Petrarca M, Béjot P, Kasparian J, Wolf J-P and Baltuška A 2013 Mid-infrared laser filamentation in molecular gases *Opt. Lett.* **38** 3194–7

[7] Weisshaupt J, Juvé V, Holtz M, Ku S, Woerner M, Elsaesser T, Ališauskas S, Pugžlys A and Baltuška A 2014 High-brightness table-top hard x-ray source driven by sub-100-femtosecond mid-infrared pulses *Nat. Photonics* **8** 927–30

[8] Serebryannikov E E and Zheltikov A M 2014 Quantum and semiclassical physics behind ultrafast optical nonlinearity in the mid-infrared: the role of ionization dynamics within the field half cycle *Phys. Rev. Lett.* **113** 043901

[9] Colosimo P *et al* 2008 Scaling strong-field interactions towards the classical limit *Nat. Phys.* **4** 386–9

[10] Haessler S *et al* 2010 Attosecond imaging of molecular electronic wavepackets *Nat. Phys.* **6** 200—206

[11] Itatani J, Levesque J, Zeidler D, Niikura H, Pépin H, Kieffer J, Corkum P and Villeneuve D 2004 Tomographic imaging of molecular orbitals *Nature* **432** 867–71

[12] Meckel M *et al* 2008 Laser-induced electron tunneling and diffraction *Science* **320** 1478–82

[13] Arnaud J A 1976 *Beam and Fiber Optics* (New York: Academic)

[14] Fock V A 1965 *Electromagnetic Diffraction and Propagation Problems* (London: Pergamon)

[15] Shen Y R 1984 *The Principles of Nonlinear Optics* (New York: Wiley-Interscience)

[16] Marburger J H 1975 Self-focusing: theory *Prog. Quantum Electron.* **4** 35–110

[17] Marcuse D 1982 *Light Transmission Optics* 2nd edn (New York: Van Nostrand Reinhold)

[18] Landau L D and Lifshitz E M 1960 *Electrodynamics of Continuous Media* (New York: Pergamon)

[19] Zheltikov A M 2013 Self-focusing and spatial modes in free space and nonlinear waveguides *Phys. Rev.* A **88** 063847

[20] Couairon A and Mysyrowicz A 2007 Femtosecond filamentation in transparent media *Phys. Rep.* **441** 47–189

[21] Berge L, Skupin S, Nuter R, Kasparian J and Wolf J-P 2007 Ultrashort filaments of light in weakly ionized, optically transparent media *Rep. Prog. Phys.* **70** 1633–713

[22] Bespalov V I and Talanov V I 1966 Filamentary structure of light beams in nonlinear liquids *JETP Lett.* **3** 307–10

[23] Campillo A J, Shapiro S L and Suydam B R 1973 Periodic breakup of optical beams due to self-focusing *Appl. Phys. Lett.* **23** 628–30

[24] Méjean G, Kasparian J, Yu J, Salmon E, Frey S, Wolf J-P, Skupin S, Vinçotte A, Nuter R, Champeaux S and Bergé L 2005 Multifilamentation transmission through fog *Phys. Rev.* E **72** 026611

[25] Salamé R, Lascoux N, Salmon E, Ackermann R, Kasparian J and Wolf J-P 2007 Propagation of laser filaments through an extended turbulent region *Appl. Phys. Lett.* **91** 171106

[26] Ettoumi W, Kasparian J and Wolf J-P 2015 Spin-glass model governs laser multiple filamentation *Phys. Rev. Lett.* **115** 033902

[27] Voronin A A, Zheltikov A M, Ditmire T, Rus B and Korn G 2013 Subexawatt few-cycle lightwave generation via multipetawatt pulse compression *Opt. Commun.* **291** 299–303

[28] Zhokhov P A and Zheltikov A M 2013 Attosecond shock waves *Phys. Rev. Lett.* **110** 183903

[29] Zhokhov P A, Panchenko V Y and Zheltikov A M 2012 Filamentation-assisted self-compression of subpetawatt laser pulses to relativistic-intensity subcycle field waveforms *Phys. Rev.* A **86** 013835